Kinase Domain Activation of FGFR2 Yields High-Grade Lung Adenocarcinoma Sensitive to a Pan-FGFR Inhibitor in a Mouse Model of NSCLC

Published in final edited form as:
Cancer Res. 2014 September 1; 74(17): 4676–4684. doi:10.1158/0008-5472.CAN-13-3218.

Kinase domain activation of FGFR2 yields high-grade lung adenocarcinoma sensitive to a pan-FGFR inhibitor in a mouse model of NSCLC

Jeremy H. Tchaicha[1,2,3], **Esra A. Akbay**[1,2,3], **Abigail Altabef**[1,3], **Oliver R. Mikse**[1,2,3], **Eiki Kikuchi**[1,2,3], **Kevin Rhee**[1,3], **Rachel G. Liao**[1,4], **Roderick T. Bronson**[5], **Lynette M. Sholl**[6], **Matthew Meyerson**[1,2,4], **Peter S. Hammerman**[1,2,4,*], and **Kwok-Kin Wong**[1,2,3,7,*]

[1]Department of Medicine, Dana Farber Cancer Institute, Boston, MA

[2]Harvard Medical School, Boston, MA

[3]Ludwig Institute for Cancer, Cambridge, MA

[4]The Broad Institute, Cambridge, MA

[5]Department of Microbiology and Immunobiology, Division of Immunology, Harvard Medical School, Boston, MA

[6]Department of Pathology, Brigham and Women's Hospital, Boston, MA

[7]Belfer Institute for Applied Cancer Science, Boston, MA

Abstract

Somatic mutations in *Fibroblast Growth Factor Receptor 2 (FGFR2)* are present in 4-5% of patients diagnosed with non-small cell lung cancer (NSCLC). Amplification and mutations in *FGFR* genes have been identified in patients with NSCLC and clinical trials are testing the efficacy of anti-FGFR therapies. *FGFR2* and other *FGFR* kinase family gene alterations have been found in both lung squamous cell carcinoma and lung adenocarcinoma though mouse models of FGFR driven lung cancers have not been reported. Here, we generated a genetically engineered mouse model (GEMM) of NSCLC driven by a kinase domain mutation in *FGFR2*. Combined with p53 ablation, primary grade III/IV adenocarcinoma was induced in the lung epithelial compartment exhibiting locally invasive and pleiotropic tendencies largely made up of multinucleated cells. Tumors were acutely sensitive to pan-FGFR inhibition. This is the first FGFR2-driven lung cancer GEMM, which can be applied across different cancer indications in a preclinical setting.

Correspondence to: Kwok-Kin Wong, Department of Medical Oncology, Dana-Farber Cancer Institute, 450 Brookline Ave, Boston, MA 02215, Kwok-Kin_Wong@dfci.harvard.edu, or, Peter S. Hammerman, Department of Medical Oncology, Dana-Farber Cancer Institute, 450 Brookline Ave, Boston, MA 02215, Peter_Hammerman@dfci.harvard.edu.
*These laboratories contributed equally.

Conflicts of interest:
M.M. was a consultant to Novartis and received research support from Novartis, and is a founding advisor and consultant to, and an equity holder in, Foundation Medicine. P.S.H. reports consulting fees from ARIAD and Eli Lilly. K.K.W. reports no conflicts.

Keywords

Fibroblast growth factor receptor 2; genetically engineered mouse models; non-small cell lung cancer; adenocarcinoma; BGJ-398

Introduction

Non-small cell lung cancer (NSCLC) currently remains the leading cause of cancer-related deaths worldwide; over 200,000 new cases are diagnosed annually, of which only 16% of patients survive longer than 5 years (1) NSCLC represents the most common subtype of lung cancer and is comprised of large cell, squamous cell and adenocarcinomas (2), all of which are being intensely researched to further delineate their respective oncogenic drivers and therapeutic targets. In turn, there is significant pre-clinical need for the development of novel genetically engineered mouse models (GEMMs) that exploit these potential 'drivers' to further understand their underlying biology and relevance as therapeutic biomarkers. Upon successful recapitulation of the human disease in the mouse, researchers are able to test novel targeted therapeutics in order to improve therapies for specific patient genotypes in NSCLC.

Fibroblast growth factors (FGFs) and their cognate cell surface receptors comprise a large signaling network, playing key roles in embryonic development and normal tissue homeostasis via ligand binding of the extracellular domains in fibroblast growth factor receptors (FGFRs). Aberrant activation of these receptor tyrosine kinases (RTKs) has been demonstrated in a variety of cancer types. To date, *FGFR1* amplification and gene expression has been the most commonly discovered, identified in 10% of breast carcinomas (3), approximately 20% of squamous cell lung cancers (4, 5), and 6% of small cell lung cancer patients (6). *FGFR2* mutations have been most highly represented in 12% of endometrial carcinoma patients (7), both major subtypes of NSCLC with the squamous cell population displaying a higher rate of mutation (8–10) and gastric tumors (11), as well. Somatic mutations in *FGFR3* have been most commonly observed in bladder carcinomas (12) and a serine to cysteine amino acid change at amino acid 249 has been identified in 5% of invasive cervical carcinomas (13). Similar to the case of *EML4-ALK*, activating chromosomal translocations of *FGFRs* have begun to be identified in several different cancer types, including bladder cancer (14), multiple myeloma (15), lung squamous cell, thyroid, oral, head and neck squamous, breast and prostate cancers as well as cholangiocarcinoma and glioblastoma. (16) *FGFR2/3/4* mutations were also identified in NSCLC (8, 9) providing the rationale for the creation of GEMMs driven by FGFR-dependent activity.

To date, several mouse models of lung tumorigenesis have been generated which are driven by different FGF7 subfamily members (FGF3/7/10). Each of these mouse models exhibited epithelial hyperplasia with some providing adenomas, but none of these models rendered an invasive cancer phenotype (17–19). More recently, a group described an inducible mouse model driven by FGF9 expression in the adult mouse lung. (20) This model was the first to develop papillary adenomas, which progressed to adenocarcinoma with the potential to

metastasize and was dependent on a FGF9-FGFR3 signaling axis. Given that FGF3/7/10 ligands predominantly signal through FGFR2 (21), the pre-clinical need for additional FGFR-driven models of invasive carcinoma is needed, as mutations in all FGFRs have been identified in various next generation sequencing efforts in various cancer indications, including NSCLC. (8, 9) Additionally, modes of resistance to tyrosine kinase inhibitors related to FGFR de-repression is also of interest. While there have been many *FGFR* mutations identified in NSCLC, limited knowledge as to which are oncogenic drivers continues to be an obstacle. As a result of data generated by TCGA analysis of lung squamous cell and adenocarcinoma, several potentially key 'drivers' were uncovered. Of those, *FGFR2* was of particular interest as it is commonly mutated and/or amplified in both lung squamous cell and adenocarcinoma patients. (8, 9) Upon further evaluation of *FGFR2*, several key mutations in both the extracellular and kinase domains showed transforming capabilities in vitro and in xenograft studies with profound sensitivity to pan-FGFR inhibitors, such as BGJ-398 and AZD4547. (22) Based on these findings and the clear void of mouse models of human lung squamous cell carcinoma, here we report the generation and characterization of FGFR2 mutant GEMMs conditionally expressing an extracellular (W290C) or kinase (K660N) domain activating mutation.

Methods

Generation and maintenance of transgenic mice

Point mutations W290C and K660N within human *FGFR2*'s cDNA (isoform IIIb) were introduced as described elsewhere. (22) In short, sequence-verified constructs were cloned into a modified transgenic targeting vector. (23) Sequence-verified targeting vectors were co-electroporated with an FLPe recombinase plasmid into v6.5 C57BL/6J (Female)×129/sv (Male) embryonic stem (ES) cells (Open Biosystems) as described elsewhere. (24) Resulting hygromycin-resistant ES clones were evaluated for transgene integration via PCR. Then, transgene positive ES clones were injected into black 6 blastocysts and resulting chimeras were mated with BALB/c WT mice to determine germline transmission of the *FGFR2* transgene. FGFR2 transgenic mice were bred with a p53 conditional knockout ($Trp53^{flox/flox}$ – Jackson Laboratories #8462) model. For all studies, mice were on a mixed genetic background and FGFR2 mutant mice were hemizygosed. Adenovirus-Cre ($5x10^7$ pfu – University of Iowa) was administered intranasally to excise the loxP sites, activating mutant FGFR2 expression and inactivating p53 activity in the lung epithelial compartment. All mouse experiments were performed with the approval of the institutional animal care and use committee at Dana-Farber Cancer Institute.

Mouse drug treatment studies

Upon signs of dyspnea, mice were imaged via magnetic resonance imaging (MRI) to document baseline tumor volumes. BGJ-398 (SelleckBio #S2183) was dosed orally 7 days/ week (15mg/kg in PEG300). (22, 25) Vehicle animals were treated with PEG300 alone (EMD). MRI was performed at 1, 2 and 4 weeks throughout treatment. Tumor volumes were quantified using 3D Slicer software as described elsewhere. (26)

Real time PCRs

Total RNA was isolated from lung tissues/nodules using Trizol (Invitrogen #15596018) and processed thru a RNA cleanup step (Qiagen #74204) per manufacturers' instructions. cDNAs were generated from resulting total RNA samples via the high-capacity RNA-cDNA kit (Invitrogen #437;7474). Real time assays were performed with real time human *FGFR2* (F: GATAAATACTTCCAATGCAGAAGTGCT R: TGCCCTATATAATTGGAGACCTTACA) or mouse *GAPDH* (F: CATGGCCTTCCGTGTTCCTA R: CCTGCTTCACCACCTTCTTGAT) primers using the Syber Green kit (Invitrogen #4364344) using 80 ng cDNA per manufacturer's instruction. Triplicates were evaluated for each sample. The ΔΔCT method was used to quantify relative mRNA quantities. Data is displayed in fold changes as compared to internal control mouse *GAPDH*.

Western Blotting and antibodies

Tumor tissues were mechanically homogenized in RIPA buffer with EDTA (Boston BioProducts) with a protease/phosphatase inhibitor cocktail (Thermo Scientific). 25 μg of total protein was separated by SDS-polyacrylamide gel electrophoresis (Invitrogen) and transferred to PVDF (Millipore). Immunoblots were probed for various proteins, including FGFR2 (C8, Santa Cruz #6930), total-FRS2a (Abcam #10425), phospho-FRS2a (Cell Sig. #3861), total-Erk1/2 (Cell Sig. #4695), phospho-Erk1/2 (Cell Sig. #4370), total-Akt (Cell Sig. #9272), phosphor-Akt (Cell Sig. #4060), and beta-actin (Cell Sig. #4967).

Immunohistochemistry and antibodies

Mouse lungs were inflated and fixed with 10% buffered formalin overnight and embedded in paraffin (FFPE). Unstained sections were stained with the following antibodies: TTF-1 (Epitomics, #58803-1), SFTPC (Chemicon, #AB378), CC-10 (Santa Cruz, #sc-9772), FGFR2 (Atlas Antibodies #HPA035305), phospho-FRS2a (Abcam #78195), and phospho-Akt/Erk1/2 (see above). Staining kits for Ki67 (Vector #VP-K451) and TUNEL (Millipore #S7100) were performed per manufacturer's instructions. Three representative images were quantified per mouse and averaged with a minimum sample size of 6 animals per cohort (treated vs. untreated).

Statistics

P-values for all survival curves were assessed by log-rank test while all other p-values were assessed by Student's T-test (GraphPad Prism).

Results

Next generation sequencing (NGS) of patient samples has been increasingly performed in order to uncover their oncogenic drivers and determine whether or not targeted therapy would be potentially more beneficial over cytotoxic therapy. We interrogated three publically available NSCLC datasets for mutation in *FGFR2* (Supplemental Table 1) (8, 9, 27). Mutations in *FGFR2* are spread across the gene, primarily focused in the extracellular or kinase domains, in NSCLC (Figure 1A). Mutations in these domains have been

previously shown to lead to constitutive receptor dimerization or kinase activity, respectively, driving oncogenic intracellular signaling. (22)

Patients with *FGFR2* mutations ranged in age from 42 to 81, averaging 66 years of age upon diagnosis. The combined data also suggested the 2:1 ratio of tumor histology (squamous cell carcinoma to adenocarcinoma) with no predilection for light to non-smokers. Due to an overwhelming need for mouse models of novel oncogenic drivers in lung cancer, we set out to evaluate newly characterized *FGFR2* mutations which were established to be transforming and oncogenic *in vitro* and *in vivo*. (22)

We generated inducible models of human *FGFR2-IIIb* mutations found in the extracellular (W290C) or kinase domains (K660N) (Supplemental Figure 1). Patients with previously reported *FGFR2* mutations were largely devoid of intact p53 activity (>85%), (9) therefore, the FGFR2 GEMMs were crossed with the $Trp53^{fl/fl}$ model to obtain a bi-allelic mouse (Figure 1B). The gain or loss of function of FGFR2 or p53, respectively, was conditional via cre-lox technology. At 6 weeks of age, bi-allelic mice were induced via intranasal delivery of adenovirus-cre (5×10^7 pfu), activating mutant FGFR2 activity while inactivating p53. Induced animals revealed a lung tumor latency of 28 to 32 weeks post adenovirus-cre administration (Figure 1B). Sick animals presented with progressive dyspnea and weight loss. As expected, bi-allelic $FGFR2^{K660N}$;$p53^{-/-}$ tumor bearing animals displayed a significant decrease in overall survival as compared to un-induced littermate controls (Figure 1C). Resulting tumors resembled poorly differentiated human grade III/IV lung adenocarcinoma displaying high pleiotropy and heavily multi-nucleated tumor cells exhibiting strong characteristics of local invasion throughout the lung parenchyma (Figure 1D). Indeed, these tumors expressed robust levels of the adenocarcinoma marker, thyroid transcription factor 1 (TTF-1) (Figure 1E). To further characterize the model, tumors were stained with surfactant protein C (SFTPC – Figure 1E) suggesting a type II pneumocyte differentiation, similarly observed in another mouse model of lung adenocarcinoma driven by FGF9. (20) These tumors stained negative for the clara cell antigen (CC10) marker at both early and late time points (20 and 32 weeks post-induction), while the clara cells of the alveolar epithelium stained positive (Supplemental Figure 2). FGFR2 mutant models displayed similar phenotypes, but the penetrance for the extracellular domain (ECD) was less than the kinase domain (KD), 35% versus 92%, respectively. Furthermore, the ECD (W290C) model's tumor latency was substantially longer than that of the K660N (KD) animals. Thus, we chose to move forward with the kinase domain mutant for treatment studies because of its increased oncogenic activity (22) and recurrent mutation in patient samples (Supplemental Table 1). Loss of p53 activity yielded increased penetrance (40% vs. 92% for *p53* wt and null, respectively) and decreased tumor latency (Supplemental Table 2).

Mutant mice developed distinct macroscopic nodules (Supplemental Figure 3) that provided for isolation from normal adjacent lung in order to molecularly characterize them, both at the RNA and protein level. Human *FGFR2* mRNA in tumor nodules was 15-20 fold higher than what was found in normal un-induced lung (Figure 2A). In general, FGF receptors signal through a key intracellular binding partner, fibroblast growth factor receptor substrate 2 alpha (FRS2α) that leads to MAPK and PI3K/Akt activity. (28) As a result of FGFR2 over-expression in our GEMM, elevated phosphorylation events in FRS2α demonstrated the

receptors increased tyrosine kinase activity, leading to increased levels of phosphorylated AKT and ERK1/2 (Figure 2B).

Next, we validated our immunoblot results via immunohistochemistry for the same downstream signaling mediators resulting from increased FGFR2 activity (Figure 2C & Supplemental Figure 4). Tumor nodules from both mutant FGFR2 models displayed robust specific cell surface staining of FGFR2. A tumor driven by mutant Kras activity showed no staining (Supplemental Figure 5A). Expected phosphorylation of various downstream signaling molecules, including AKT, ERK1/2 and FRS2α were present in tumor nodules from both the kinase domain mutant (Figure 2C) and the extracellular domain mutant (Supplemental Figure 4). Both models were deemed proliferative and actively growing as a result of positive Ki-67 immunohistochemistry.

Until relatively recently, the standard of care for advanced NSCLC patients has been limited to cytotoxic chemotherapy when surgery and radiotherapy were otherwise ineffective. (29) With the boom of targeted therapy driving patient sub-stratification, we wanted to evaluate the effect of a pan FGFR inhibitor in our FGFR2 driven lung cancer model. In a tumor efficacy study, we treated $FGFR2^{K660N};p53^{-/-}$ lung tumor bearing animals with either BGJ-398 (n=10), a pan FGFR inhibitor or vehicle (n=5). Tumors were confirmed via MRI and served as baseline tumor volume. After one week of treatment with daily, orally delivered 15mg/kg BGJ-398, eight of ten animals displayed greater than 50% tumor regression and three of ten animals had regressed 80% (Figure 3A, B). This phenomenon is very similar to the efficacy of erlotinib in our mutant EGFR-driven lung cancer mouse model. (30) Efficacy of BGJ-398 continued to significantly improve at 2 and 4 weeks as compared to vehicle treated animals (Figure 3C), where animals showed near remission with eight of ten animals showing greater than 75% tumor regression (Supplemental Figure 5B). Long-term sustained tumor remission is being evaluated with no acquired resistance seen at 6 months (n=4) (data not shown).

Next, we investigated the changes in downstream signaling pathways as a result of BGJ-398 treatment. Lung tumor bearing mice were treated for two days with either vehicle or BGJ-398 (15 mg/kg) and sacrificed 2 hours after the second dose to evaluate the drug's pharmacodynamics. Isolated tumor nodules from both vehicle and drug treatment arms were evaluated for phosphorylated FRS2α, AKT and ERK proteins. (31) Overall, inhibition of FGFR2-dependent tyrosine kinase activity reduced MAPK and PI3K signaling (Figure 4A) with obvious phosphorylation depletion in key signaling proteins FRS2α, AKT and ERK1/2. As a result of short term dosing, BGJ-398 treated tumors displayed signs of decreased proliferation (Ki-67) and increased apoptosis (TUNEL) via immunohistochemistry (Figure 4B). Moreover, there was a significant overall survival benefit of animals undergoing BGJ-398 treatment (n=12) compared to an untreated, induced group (n=30) (Figure 4C). Animals died on treatment due to issues unrelated to lung tumor or drug toxicity, most commonly due to improper oral dosing (n=2) or a secondary tumor arising in the nasal airway epithelia that commonly metastasized to the brain (Supplemental Figure 6). Unlike the tumors originating in the lungs, these FGFR2 positive nasal tumors were negative for the type II pneumocyte marker SFTPC (Supplemental Figure 6). After review, a Veterinary Pathologist termed these esthesioneuroblastomas (n=2, Supplemental Figure 6), arising from

the neuroepithelium. These tumors developed well beyond the normal lung tumor latency (> 50 weeks), likely as a direct result of nasally delivered adenovirus cre and resulted in lethality due to obstruction of the nasal cavity, affecting the animal's normal respiration. BGJ-398 caused a significant decrease in proliferation (Figure 4D) and a significant increase in apoptosis of the lung tumor cells (Figure 4E) after a short-term (2 day) treatment resulting in near complete tumor regression at four weeks.

Discussion

FGF ligands and their cognate receptors have become significant clinical targets of interest in the oncology field. Recently, a group reported an inducible mouse model driving FGF9 expression in the adult airway epithelia leading to the formation of papillary adenomas, which were shown to progress into primary adenocarcinomas with a metastatic potential. (20) The FGF9 expression signaled through the FGFR3 receptor and once the tumors were established, they were shown to be FGF9-independent. Furthermore, while widespread expression of FGF3 and FGF7 in the adult mouse lung was shown to produce type II cell hyperplasia (18, 19), FGF9 or FGF10 expression led to the development of cancer or adenomas, respectively. (17, 20) Interestingly, the FGF7 subfamily of ligands (FGF3, 7, 10) is known to preferentially bind FGFR2 receptors, while FGF9 has been shown to signal through FGFR3 (21) suggesting both receptors are important in lung tumor development.

Activating mutations in FGFR2 have recently been unveiled as novel targets in NSCLC, both in lung squamous cell and adenocarcinoma. (8, 9) Inherent in their clinical relevance, models driven by FGFR2 activating mutations have the potential to help researchers explore the biology of the receptor tyrosine kinase and to evaluate novel targeted therapies for patients that fall into this genetically defined subset of cancers. A multitude of FGFR2 mutations have been identified in NSCLC, although it has been unclear as to which are, in fact, oncogenic drivers up until recently. (22) In addition, with the recent success of targeted therapies in lung adenocarcinoma patients, it would be advantageous to develop novel models of FGFR-driven lung squamous cell carcinoma (SqCC) given the prevalence of FGFR alterations in this disease.

Described herein, we have developed the first FGFR2-driven genetically engineered mouse model (GEMM) of NSCLC. We developed conditional bi-allelic mice that upon exposure to nasally delivered adenovirus-cre led to activated FGFR2 signaling, while also abrogating p53 function concurrently. Both mutant models that were developed yielded primary grade III/IV lung adenocarcinoma that led to a significant decrease in overall survival as compared to un-induced control littermates. While p53 loss of function was not required for tumor formation (Supplemental Table 2), it was necessary to provide reasonable tumor latency for long-term efficacy studies to be completed. Combining loss of p53 with constitutive FGFR2 signaling led to a marked reduction in tumor latency, also observed in a KRAS driven mouse model of lung cancer. (32) Furthermore, combining loss of p53 in our model is clinically relevant given the high frequency of p53 loss in lung cancers. (8, 9)

Unlike the FGF9 model where the oncogene is broadly expressed in all cells expressing SFTPC throughout the lung, our system targets a smaller number of epithelial cells of

diverse lineages via expression of Cre recombinase by nasal inhalation of adenovirus. This difference in technique may explain the shorter latency in previously described models. (17, 20) Differences in latency are possibly also due to overexpression of FGF ligands in previous models versus expression of the mutant receptor in this model. Ligands can have non-cell autonomous effects on the other cells in the tumor microenvironment such as endothelial cells (33) or cancer associated fibroblasts (34, 35), likely supporting the growth of these tumors. In contrast to the previously described FGF9 model, early or late lesions in our FGFR2 model lack CC-10 staining, potentially indicating a non clara cell origin though additional work is required to discover the cell of origin in these tumors (Supplemental Figure 2).

This FGFR2-driven GEMM of NSCLC was created to study the development and clinical aspects of lung cancer; however previously established mouse models overexpressing different FGFs in the lung show similar but also distinct phenotypes to the current model. The proliferative phenotypes in the FGF7 subfamily models are dependent on sustained FGF signaling (17–19) while the FGF9 model develops ligand independence upon tumor formation via FGFR3 signaling. (20)

As expected, lung tumors driven via constitutive FGFR2 signaling displayed increased AKT and ERK activity correlating with FRS2α phosphorylation. As the extracellular domain model had longer tumor latency, we chose to test BGJ-398, a pan-FGFR inhibitor, in our kinase mutant model. This model displayed exquisite sensitivity to BGJ-398 just after one week of dosing. By four weeks after dose commencement, a large majority of tumor bearing animals had undergone nearly full tumor remission lending to significantly longer overall survival compared to untreated lung tumor bearing animals. This sustained response was durable and strikingly resembled our study of EGFR tyrosine kinase inhibitors in mutant EGFR-driven mouse lung cancers. (30) There was a small group of BGJ-treated animals that died of improper oral dosing or tumors arising in the nasal epithelia. The animals showing near complete lung tumor remission developed SFTPC negative nasal tumors that protruded into the brain while also impeding upon the animal’s breathing capacity. The lack of type II alveolar marker staining (SFTPC) in these tumors confirms that they are not a result of lung metastasis. We have adapted an intratracheal delivery method to circumvent this issue in the future. While we cannot unequivocally suggest why the BGJ-398 had no therapeutic effect on these tumors, a proper drug pharmacokinetic and pharmacodynamic study would be beneficial to assess the drugs capability to penetrate the blood brain barrier.

Although the mutations in *FGFR2* were identified in an SqCC patient population, elevated FGFR2-related activity is seen across both major subtypes of NSCLC. While we set out to develop a mouse model that recapitulates human FGFR2-driven NSCLC, we were not surprised by the adenocarcinoma phenotype as the pre-clinical space is largely devoid of a lung SqCC mouse model for many potential reasons. First, when inducing oncogene expression in the mouse lung, targeting is largely directed to type II pneumocytes (alveolar type II cells), which have a predilection to lead to bronchio-alveolar adenomas leading to lung adenocarcinoma. (36) Furthermore, the naïve mouse lung epithelium has no squamous cell differentiation until an inflammatory event occurs driving metaplasia, which is often initiated in SqCC patients by smoking. (37) Recently, a group has shown the necessity for

chronic inflammation to drive spontaneous SqCC formation within the mouse lung. They reported inactivation of IKKα (kinase-dead IKKα knock-in) drives the up-regulation of SqCC-associated markers including p63, Trim29 and keratin 5 leading to down-regulation of LKB1 (STK11) activity. (38) Second, there are likely several features of the microenvironment that are playing roles in squamous cell differentiation which a transgenic environment would have difficulty recapitulating without that initial inflammatory insult. Third, there is also a strong possibility that those patients with *FGFR2* mutations may require another collaborating oncogene to drive the differentiation into the squamous cell histology, or perhaps the loss of another tumor suppressor.

In summary, we have developed a mouse model of lung adenocarcinoma driven by FGFR2 constitutive kinase activation originally identified in NSCLC patients. With the exquisite sensitivity of the lung tumor model to a pan-FGFR inhibitor, researchers gain a powerful tool to further bolster their understanding of FGFR-related cancer biology and targeted therapy discovery within the lung and across various cancer indications. In addition, with the inevitability of acquired resistance, this model could be of significant value for evaluation of response to targeted therapies, chemotherapy as well as novel immunotherapies in an immune-competent environment. Together, these data validate a role for FGFR2 in lung adenocarcinoma providing a model to further make an impact in the decisions made by an oncologist treating this genetically defined population in the clinic.

Supplementary Material

Refer to Web version on PubMed Central for supplementary material.

Acknowledgments

We thank Christine Lam for tissue processing and Mei Zhang for help with immunohistochemistry. Lina Du kindly performed the blastocyst injections for transgenic generation in Dr. Arlene Sharpe's lab at Harvard Medical School.

Financial Disclosures:

P.S.H. is supported by NCI grants 1K08CA163677, and the Stephen D. and Alice Cutler Investigator Fund. M.M. is supported by United against Lung Cancer, the Lung Cancer Research Foundation, the American Lung Association, Novartis Pharmaceuticals and NCI grant P50CA090578. K.K.W. is supported by the NIH (CA122794, CA140594, CA163896, CA166480, CA154303, CA120964), United against Lung Cancer and the American Lung Association.

References

1. Wao H, Mhaskar R, Kumar A, Miladinovic B, Djulbegovic B. Survival of patients with non-small cell lung cancer without treatment: a systematic review and metaanalysis. Systematic reviews. 2013; 2:10. [PubMed: 23379753]
2. Herbst RS, Heymach JV, Lippman SM. Lung cancer. N Engl J Med. 2008; 359:1367–1380. [PubMed: 18815398]
3. Elbauomy Elsheikh S, Green AR, Lambros MB, Turner NC, Grainge MJ, Powe D, et al. FGFR1 amplification in breast carcinomas: a chromogenic in situ hybridisation analysis. Breast cancer research : BCR. 2007; 9:R23. [PubMed: 17397528]
4. Dutt A, Ramos AH, Hammerman PS, Mermel C, Cho J, Sharifnia T, et al. Inhibitor-sensitive FGFR1 amplification in human non-small cell lung cancer. PLoS One. 2011; 6:e20351. [PubMed: 21666749]

5. Tran TN, Selinger CI, Kohonen-Corish MR, McCaughan BC, Kennedy CW, O'Toole SA, et al. Fibroblast growth factor receptor 1 (FGFR1) copy number is an independent prognostic factor in non-small cell lung cancer. Lung cancer. 2013; 81:462–467. [PubMed: 23806793]
6. Schultheis AM, Bos M, Schmitz K, Wilsberg L, Binot E, Wolf J, et al. Fibroblast growth factor receptor 1 (FGFR1) amplification is a potential therapeutic target in smallcell lung cancer. Modern pathology : an official journal of the United States and Canadian Academy of Pathology, Inc. 2013
7. Dutt A, Salvesen HB, Chen TH, Ramos AH, Onofrio RC, Hatton C, et al. Drug-sensitive FGFR2 mutations in endometrial carcinoma. Proceedings of the National Academy of Sciences of the United States of America. 2008; 105:8713–8717. [PubMed: 18552176]
8. Imielinski M, Berger AH, Hammerman PS, Hernandez B, Pugh TJ, Hodis E, et al. Mapping the hallmarks of lung adenocarcinoma with massively parallel sequencing. Cell. 2012; 150:1107–1120. [PubMed: 22980975]
9. Cancer Genome Atlas Research N. Comprehensive genomic characterization of squamous cell lung cancers. Nature. 2012; 489:519–525. [PubMed: 22960745]
10. Davies H, Hunter C, Smith R, Stephens P, Greenman C, Bignell G, et al. Somatic mutations of the protein kinase gene family in human lung cancer. Cancer research. 2005; 65:7591–7595. [PubMed: 16140923]
11. Jang JH, Shin KH, Park JG. Mutations in fibroblast growth factor receptor 2 and fibroblast growth factor receptor 3 genes associated with human gastric and colorectal cancers. Cancer research. 2001; 61:3541–3543. [PubMed: 11325814]
12. Gust KM, McConkey DJ, Awrey S, Hegarty PK, Qing J, Bondaruk J, et al. Fibroblast growth factor receptor 3 is a rational therapeutic target in bladder cancer. Mol Cancer Ther. 2013; 12:1245–1254. [PubMed: 23657946]
13. Rosty C, Aubriot MH, Cappellen D, Bourdin J, Cartier I, Thiery JP, et al. Clinical and biological characteristics of cervical neoplasias with FGFR3 mutation. Molecular cancer. 2005; 4:15. [PubMed: 15869706]
14. Williams SV, Hurst CD, Knowles MA. Oncogenic FGFR3 gene fusions in bladder cancer. Human molecular genetics. 2013; 22:795–803. [PubMed: 23175443]
15. Kalff A, Spencer A. The t(4;14) translocation and FGFR3 overexpression in multiple myeloma: prognostic implications and current clinical strategies. Blood cancer journal. 2012; 2:e89. [PubMed: 22961061]
16. Wu YM, Su F, Kalyana-Sundaram S, Khazanov N, Ateeq B, Cao X, et al. Identification of targetable FGFR gene fusions in diverse cancers. Cancer Discov. 2013; 3:636–647. [PubMed: 23558953]
17. Clark JC, Tichelaar JW, Wert SE, Itoh N, Perl AK, Stahlman MT, et al. FGF-10 disrupts lung morphogenesis and causes pulmonary adenomas in vivo. American journal of physiology Lung cellular and molecular physiology. 2001; 280:L705–L715. [PubMed: 11238011]
18. Tichelaar JW, Lu W, Whitsett JA. Conditional expression of fibroblast growth factor-7 in the developing and mature lung. The Journal of biological chemistry. 2000; 275:11858–11864. [PubMed: 10766812]
19. Zhao B, Chua SS, Burcin MM, Reynolds SD, Stripp BR, Edwards RA, et al. Phenotypic consequences of lung-specific inducible expression of FGF-3. Proceedings of the National Academy of Sciences of the United States of America. 2001; 98:5898–5903. [PubMed: 11331772]
20. Yin Y, Betsuyaku T, Garbow JR, Miao J, Govindan R, Ornitz DM. Rapid Induction of Lung Adenocarcinoma by Fibroblast Growth Factor 9 Signaling through FGF Receptor-3. Cancer research. 2013; 73:5730–5741. [PubMed: 23867472]
21. Zhang X, Ibrahimi OA, Olsen SK, Umemori H, Mohammadi M, Ornitz DM. Receptor specificity of the fibroblast growth factor family. The complete mammalian FGF family. The Journal of biological chemistry. 2006; 281:15694–1700. [PubMed: 16597617]
22. Liao RG, Jung J, Tchaicha J, Wilkerson MD, Sivachenko A, Beauchamp EM, et al. Inhibitor-Sensitive FGFR2 and FGFR3 Mutations in Lung Squamous Cell Carcinoma. Cancer research. 2013

23. Chen Z, Sasaki T, Tan X, Carretero J, Shimamura T, Li D, et al. Inhibition of ALK, PI3K/MEK, and HSP90 in murine lung adenocarcinoma induced by EML4-ALK fusion oncogene. Cancer research. 2010; 70:9827–9836. [PubMed: 20952506]
24. Beard C, Hochedlinger K, Plath K, Wutz A, Jaenisch R. Efficient method to generate single-copy transgenic mice by site-specific integration in embryonic stem cells. Genesis. 2006; 44:23–28. [PubMed: 16400644]
25. Guagnano V, Furet P, Spanka C, Bordas V, Le Douget M, Stamm C, et al. Discovery of 3-(2,6-dichloro-3,5-dimethoxy-phenyl)-1-{6-[4-(4-ethyl-piperazin-1-yl)-phenylamin o]-pyrimidin-4-yl}-1-methyl-urea (NVP-BGJ398), a potent and selective inhibitor of the fibroblast growth factor receptor family of receptor tyrosine kinase. J Med Chem. 54:7066–7083. [PubMed: 21936542]
26. Chen Z, Cheng K, Walton Z, Wang Y, Ebi H, Shimamura T, et al. A murine lung cancer co-clinical trial identifies genetic modifiers of therapeutic response. Nature. 2012; 483:613–617. [PubMed: 22425996]
27. Kim Y, Hammerman PS, Kim J, Yoon JA, Lee Y, Sun JM, et al. Integrative and comparative genomic analysis of lung squamous cell carcinomas in East Asian patients. J Clin Oncol. 2014; 32:121–128. [PubMed: 24323028]
28. Turner N, Grose R. Fibroblast growth factor signalling: from development to cancer. Nature reviews Cancer. 2010; 10:116–129.
29. Wakelee H, Belani CP. Optimizing first-line treatment options for patients with advanced NSCLC. The oncologist. 2005; 10(Suppl 3):1–10. [PubMed: 16368866]
30. Ji H, Li D, Chen L, Shimamura T, Kobayashi S, McNamara K, et al. The impact of human EGFR kinase domain mutations on lung tumorigenesis and in vivo sensitivity to EGFR-targeted therapies. Cancer cell. 2006; 9:485–495. [PubMed: 16730237]
31. Dailey L, Ambrosetti D, Mansukhani A, Basilico C. Mechanisms underlying differential responses to FGF signaling. Cytokine & growth factor reviews. 2005; 16:233–247. [PubMed: 15863038]
32. Jackson EL, Olive KP, Tuveson DA, Bronson R, Crowley D, Brown M, et al. The differential effects of mutant p53 alleles on advanced murine lung cancer. Cancer research. 2005; 65:10280–10288. [PubMed: 16288016]
33. Murakami M, Nguyen LT, Zhuang ZW, Moodie KL, Carmeliet P, Stan RV, et al. The FGF system has a key role in regulating vascular integrity. The Journal of clinical investigation. 2008; 118:3355–3366. [PubMed: 18776942]
34. Gotoh N. Control of stemness by fibroblast growth factor signaling in stem cells and cancer stem cells. Current stem cell research & therapy. 2009; 4:9–15. [PubMed: 19149625]
35. Kalluri R, Zeisberg M. Fibroblasts in cancer. Nature reviews Cancer. 2006; 6:392–401.
36. Meuwissen R, Berns A. Mouse models for human lung cancer. Genes & development. 2005; 19:643–664. [PubMed: 15769940]
37. Dakir EH, Feigenbaum L, Linnoila RI. Constitutive expression of human keratin-14 gene in mouse lung induces premalignant lesions and squamous differentiation. Carcinogenesis. 2008; 29:2377–2384. [PubMed: 18701433]
38. Xiao Z, Jiang Q, Willette-Brown J, Xi S, Zhu F, Burkett S, et al. The pivotal role of IKKalpha in the development of spontaneous lung squamous cell carcinomas. Cancer cell. 2013; 23:527–540. [PubMed: 23597566]

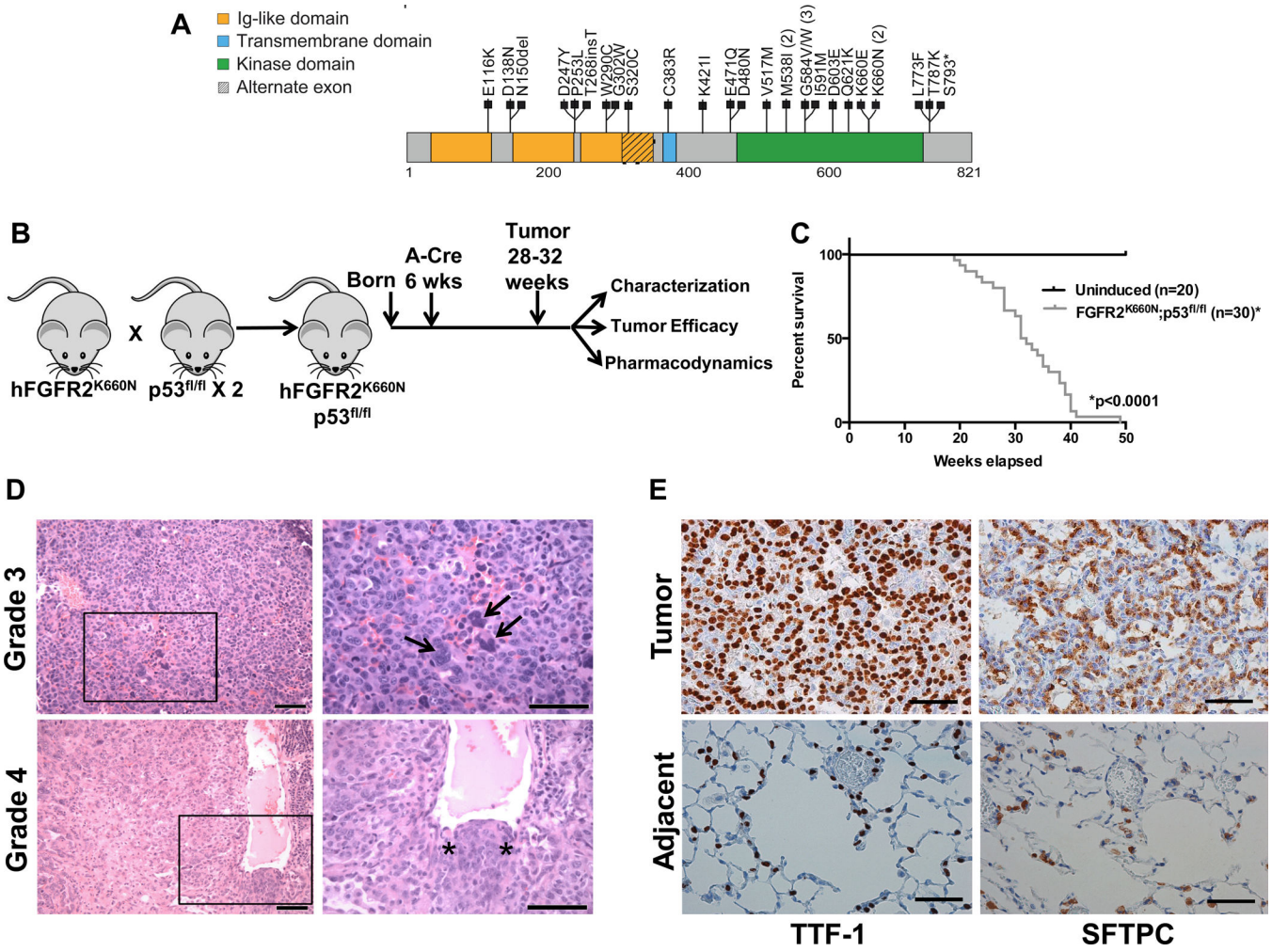

Figure 1. Kinase domain activation of FGFR2 drives the formation of grade III/IV lung adenocarcinoma in a GEMM of NSCLC

(A) Recurrent *FGFR2* mutations observed in lung adenocarcinoma and squamous cell carcinoma patient primary tumor biopsies. (B) A GEMM conditionally expressing human $FGFR2^{K660N}$ was crossed (two generations) with a conditional p53 inactivating GEMM to obtain a $FGFR2^{K660N};p53^{fl/fl}$ mouse. Compound conditional mutant animals were induced at 6 weeks of age via nasally delivered adenovirus-cre. Tumor latency ranged from 28-32 weeks post-induction. (C) *FGFR2* kinase domain mutation (n=30) significantly ($p<0.0001$) reduced the overall survival of animals as compared to un-induced littermate controls (n=20). (D) Two representative H&E images of poorly differentiated lung adenocarcinoma. Note the upper panel represents grade III lung adenocarcinoma displaying pleomorphic nuclei (arrows) and the lower panel represents grade IV lung adenocarcinoma exhibiting tumor cells invading towards the blood vessel (asterisks) (left/right panel magnification bars = 100 μM and 50 μM, respectively). (E) Tumors exhibited robust expression of TTF-1, a marker for adenocarcinoma as well as surfactant protein C (SFTPC). Adjacent non-malignant regions display basal levels of both markers (magnification bars = 50 μM).

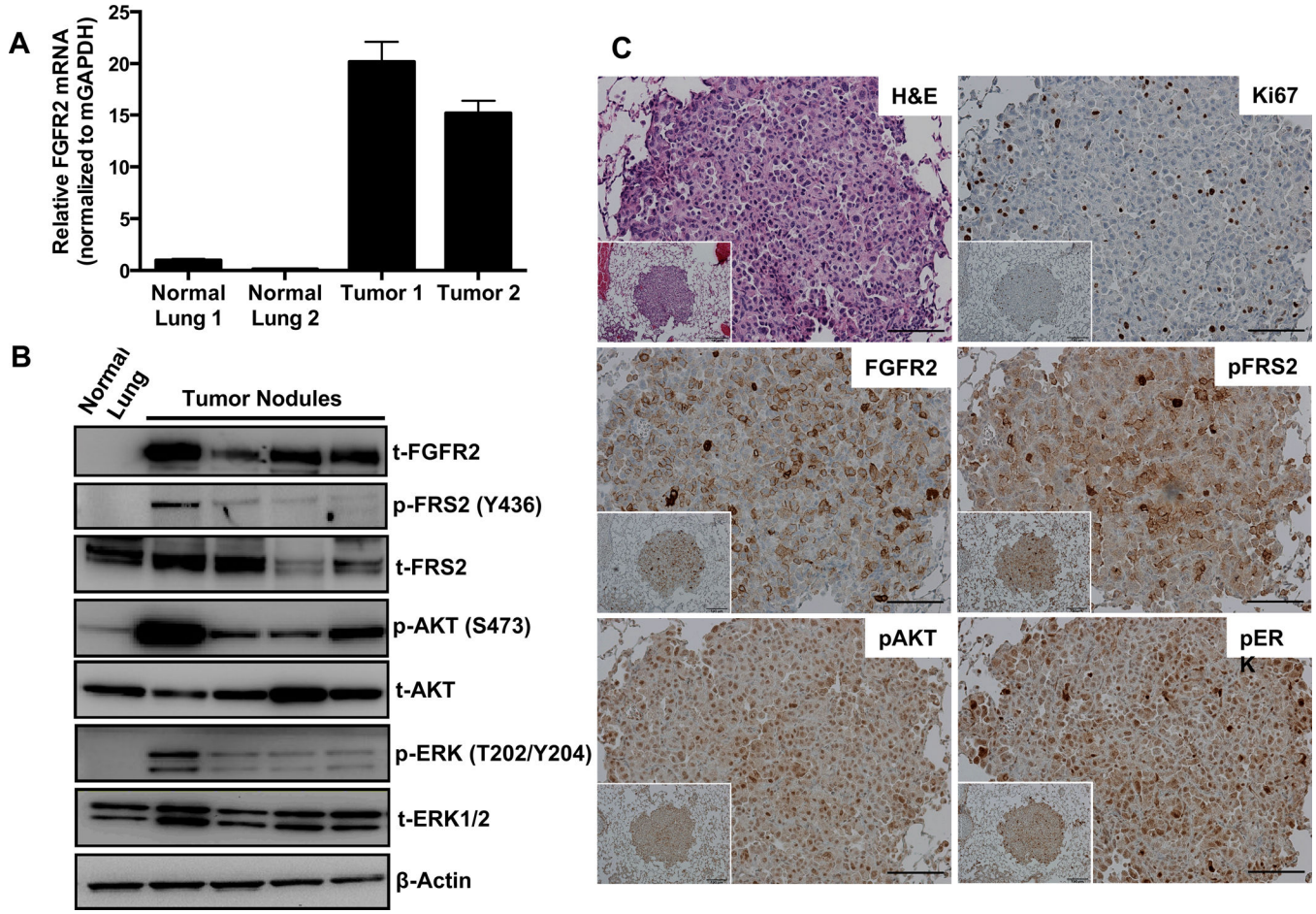

Figure 2. Conditional activation of FGFR2^{K660N} and inactivation of p53 in the lung compartment drives expression of FGFR2 and its intracellular signaling counterparts

(A) 15-20 fold higher *FGFR2* mRNA levels were observed in tumors driven by conditional activation of the bi-allelic GEMM as compared to normal lung controls (normalized to mouse *GAPDH*). (B) Expression of FGFR2, FRS2, pFRS2 (Y436), AKT, pAKT (S473), ERK, and pERK1/2 (T202/Y204) by western blot. Tumor nodules from four different mice and a control mouse lung are shown. β-actin was run as a loading control. (C) Representative images from H&E staining and immunohistochemistry for Ki-67, FGFR2, and phosphorylated forms of FRS2α, AKT, and ERK on FFPE sections of the same tumor nodule shown at low and high magnifications (inset image scale bar = 100uM, high magnification scale bar = 50uM).

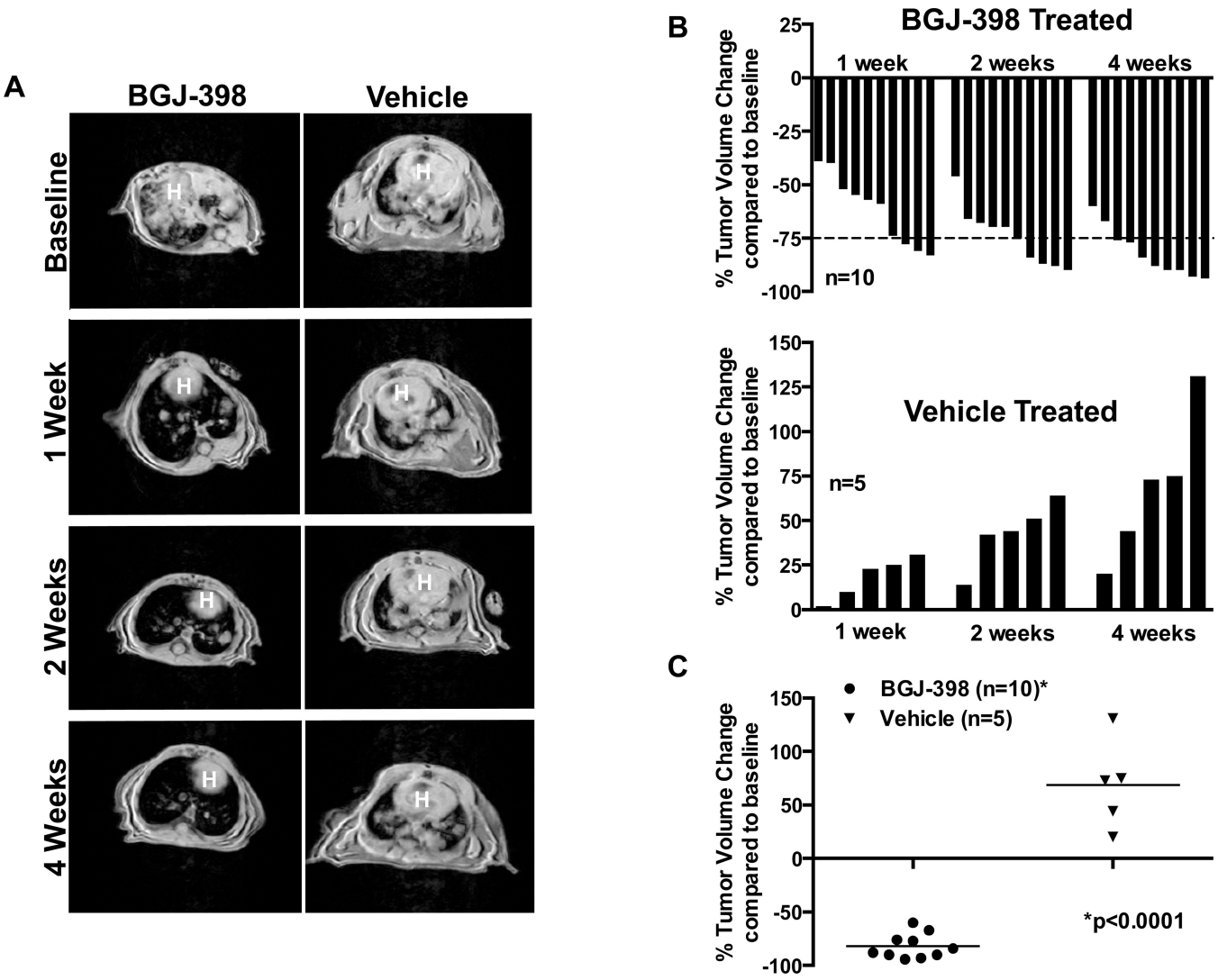

Figure 3. Pan-FGFR inhibitor, BGJ-398, is effective against FGFR2-driven lung adenocarcinoma in a genetically engineered mouse model

(A) Representative serial MR images of two $FGFR2^{K660N}$;$p53^{-/-}$ lung tumor bearing mice treated once daily for four weeks with either BGJ-398 (15 mg/kg) or vehicle (PEG300). Images represent baseline, one, two and four weeks after start of treatment (White 'H' indicates the heart). (B) Quantification of tumor burden from the MR images in BGJ-398 (upper waterfall plot) or vehicle (lower waterfall plot) treated mice at 1, 2, and 4 weeks after the start of treatment. (C) Comparison of tumor volume changes in BGJ-398 or vehicle treated mice at 4 weeks after the start of treatment ($p<0.0001$) (n=10 and 4 respectively).

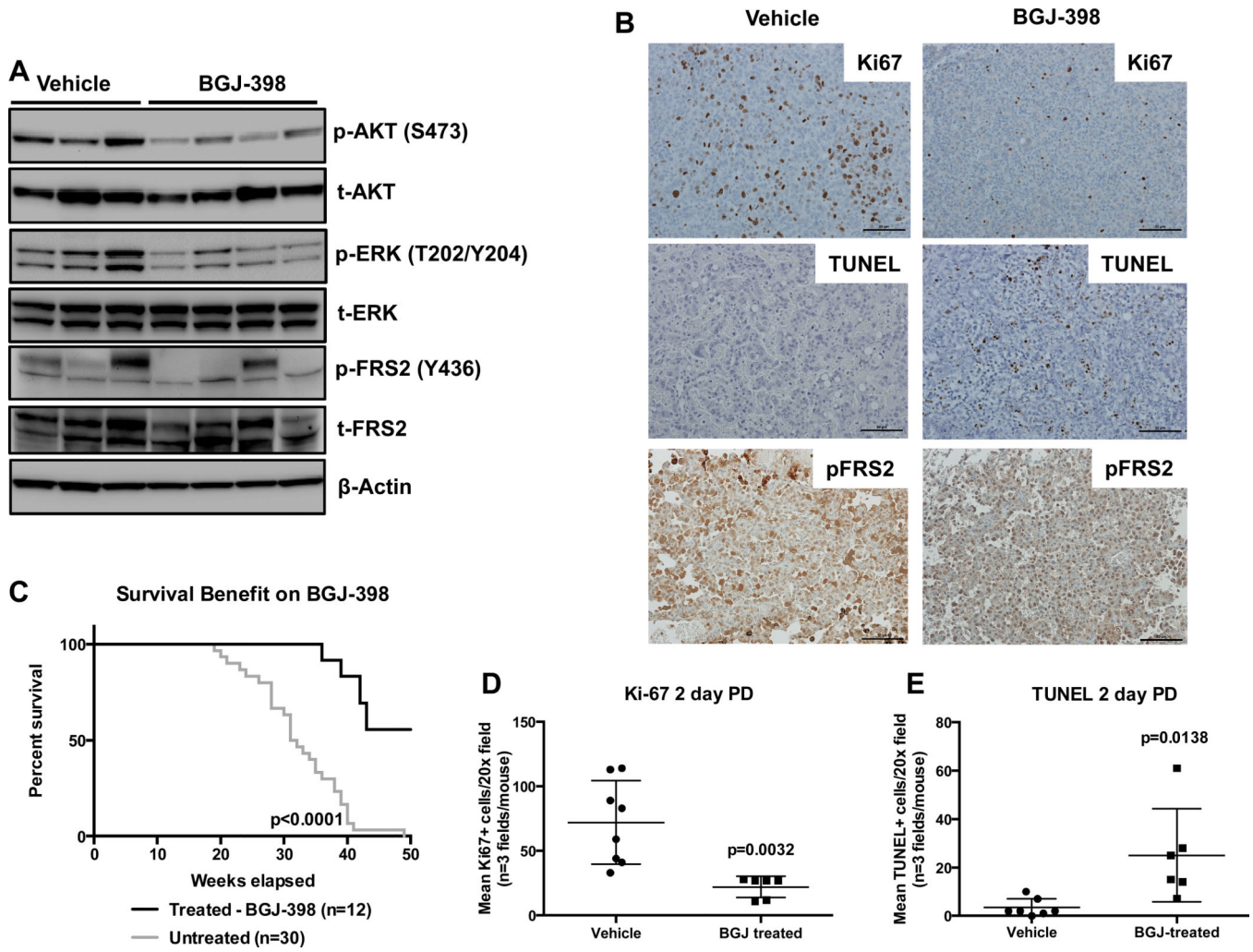

Figure 4. BGJ-398 increases the survival benefit via abrogation of key intracellular signaling cascades leading to decreased proliferation and increased cell death

(A) Western blot analysis showing pharmacodynamic markers of the canonical FGFR signaling pathway; phosphorylated protein levels of AKT (S473), ERK (T202, Y204), and FRS2α (Y436) in BGJ-398 or vehicle treated mouse lung tumor nodules. Respective total proteins and β-actin westerns were also performed as loading controls. Each lane represents a tumor nodule from a different mouse. (B) Representative images of Ki-67, pFRS2 and TUNEL IHC staining on FFPE slides of tumor nodules from mice treated for three days either with BGJ-398 or vehicle (scale bar = 50μM). (C) BGJ-398 treated (n=12) lung tumor bearing animals survive significantly ($p<0.0001$) longer than untreated, induced lung tumor bearing animals (n=30) with some (n=4) succumbing to non-tumor related deaths (see results). Mean Ki-67 (D) or TUNEL (E) positive cells per 20X field (n=3/mouse) show a significant decrease in proliferation ($p=0.0032$) and significant increase in apoptosis ($p=0.0138$) in the BGJ-398 treated cohort. [Ki-67 study – n=8/6 (vehicle/BGJ-398) and TUNEL study – n=7/6 (vehicle/BGJ-398)].